Water Production of Comet C/1999 S4 (LINEAR) Observed with the SWAN Instrument

J. Teemu T. Mäkinen,[1*] Jean-Loup Bertaux,[2] Michael R. Combi,[3] Eric Quémerais[2]

The SWAN (Solar Wind ANisotropies) Lyman-alpha all-sky camera on the SOHO spacecraft observed the hydrogen coma of comet C/1999 S4 (LINEAR) from the end of May through mid-August 2000. A systematic set of water-production rates was obtained for this well-documented event of complete fragmentation of a cometary nucleus. The observations indicate that the lower limit for the sunlit surface area of the nucleus was about 1 square kilometer before the fragmentation and that the amount of water released throughout the observing period was 3.3×10^9 kilograms. Evidence suggests that the activity of the comet was dominated by successive fragmentation. There were four major outbursts, occurring about every 16 days. The 21 July event led to the complete fragmentation and sublimation of what remained of the nucleus, producing the last 3×10^8 kilograms of water. A model where the fragment size distribution follows the power law $N(R) \sim R^{-2.7}$, where N and R are the number and radius of fragments, reproduces the observed dissipation. This distribution possibly reflects the internal structure of the nucleus.

Comets are icy remnants of the original Solar Nebula from which the solar system was formed. The Oort cloud (*1*) on the outer rim of the solar system is the main source of long-period comets. Some comets are occasionally perturbed into the inner solar system where their icy surface starts to evaporate, forming a tenuous atmosphere known as the coma. Being very small and dark, the actual nucleus of the comet is extremely difficult to observe. Thus, our best knowledge about the size and activity of a comet is obtained through observations of cometary water production, ordinary water being the most abundant volatile component in the coma. Furthermore, the internal structure of a cometary nucleus is still poorly known. Unable to probe it directly, we depend on occasional splittings of active comets for hints about the structure and composition of a comet. In this respect, the well-documented complete disintegration of comet C/1999 S4 (LINEAR) provided a valuable opportunity to refine our understanding of comets.

We present here the observations made with the SWAN (Solar Wind ANisotropies) instrument (*2*). Located on the SOHO (SOlar and Heliospheric Observatory) spacecraft, SWAN is a scanning imager operating at the ultraviolet Lyman-alpha wavelength of fluorescent neutral H at 121.6 nm. As indicated by its name, the main scientific objective of SWAN is to detect anisotropies in the solar wind as reflected in the cavity it carves into the surrounding cloud of interstellar H (*3*). In addition, SWAN is a unique tool for cometary studies because of two features. First, SWAN is capable of mapping the whole sky in 1 day. Therefore, all comets above the sensitivity limit of the instrument are routinely observed without a priori knowledge about their existence. This has so far resulted in the discovery of one new comet (*4*), and a recent study has shown that the SWAN data contain prediscovery observations for about half of the recent bright comets (*5*). Second, situated at the first Lagrangian point between Earth and the Sun, SWAN is completely free of any atmospheric or exospheric disturbances. Therefore, the consistency of measurements throughout an observing program is extremely high.

The SWAN instrument consists of two identical sensor units with a periscope mechanism that enables them to cover the northern and southern ecliptic hemispheres, respectively. Each unit has an instantaneous field-of-view (FOV) of 5° by 5° and a spatial resolution of 1° by 1°. In the full-sky mode, the line-of-sight is moved 2.5° between 13-s exposures until the whole sky has been covered. In a comet-specific observation, a 20° by 20° area around the center of the comet is similarly swept with 0.5° stepping. A cometary coma consists of an inner collision zone and an outer sphere of radially expanding gas that is usually well within the SWAN observing window. This was always the case with comet C/LINEAR. Water-production estimates based on observations of the outer coma are less model-dependent than values obtained from inner-coma observations because of the predictable nature of the H-atom velocity distribution outside the collision zone (*6*), which is too small to be resolved in SWAN images. The entire H coma represents 2 to 3 days' worth of cometary outgassing activity, and production rates given below are average values over such a period. This ensures that short-lived activity peaks cannot alter estimates of the total mass of sublimated water. Furthermore, SWAN provides a method for estimating short-term solar Lyman-alpha irradiance variations (*7*). The variations were observed at different areas of the background field, and the obtained profiles were interpolated to the location of the comet, taking into account solar rotation.

Comet C/LINEAR was anticipated to become one of the brightest comets of the year 2000. Because of the coarse spatial resolution of SWAN, the comet was not detected until late May, when it was 1.36 astronomical units (AU) from the Sun and 2.1 AU from SOHO. After 25 May the observing geometry became more favorable, resulting in estimates of the water-production rate Q_{H_2O} from 25 May until 12 August. In addition to 13 specific observations of C/LINEAR (Fig. 1), the comet was also visible on 31 full-sky maps (Table 1). All observations were compared to a basic Haser model (*8*, *9*) with equivalent scale

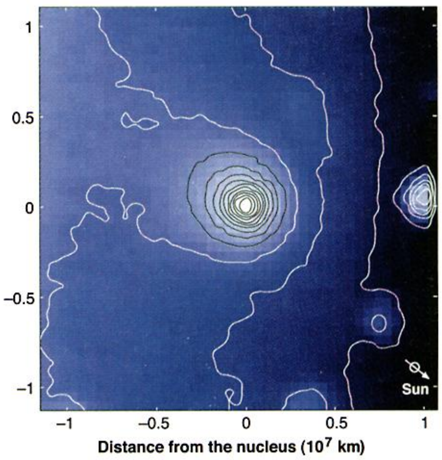

Fig. 1. Hydrogen coma of comet C/LINEAR seen by SWAN on 26 June 2000. The comet was at a distance of 0.765 AU from the Sun and 0.402 AU from SOHO. The contours are separated by 50 Rayleigh intervals with a peak intensity at ~700 Rayleigh. The coma is somewhat elongated in the anti-sunward direction but otherwise featureless.

[1]Finnish Meteorological Institute, Geophysics Research, Post Office Box 503, FIN-00101 Helsinki, Finland. [2]CNRS, Service d'Aéronomie, BP 3, 91371 Verrières le Buisson Cedex, France. [3]Space Physics Research Laboratory, University of Michigan, 2455 Hayward Street, Ann Arbor, MI 48109–2143, USA.

*To whom correspondence should be addressed. E-mail: teemu.makinen@fmi.fi

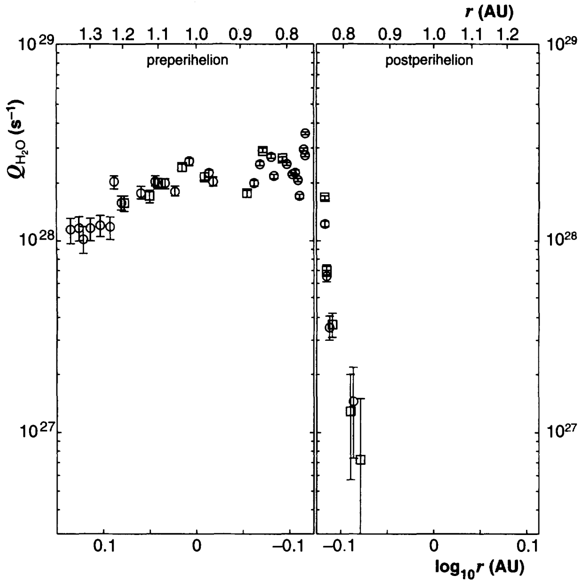

Fig. 2. The water-production rate of C/LINEAR as a function of heliocentric distance. Full-sky observations are denoted by circles and comet-specific ones with squares. The preperihelion behavior is apparently regular, but the steep postperihelion decrease reveals the fragile nature of the nucleus.

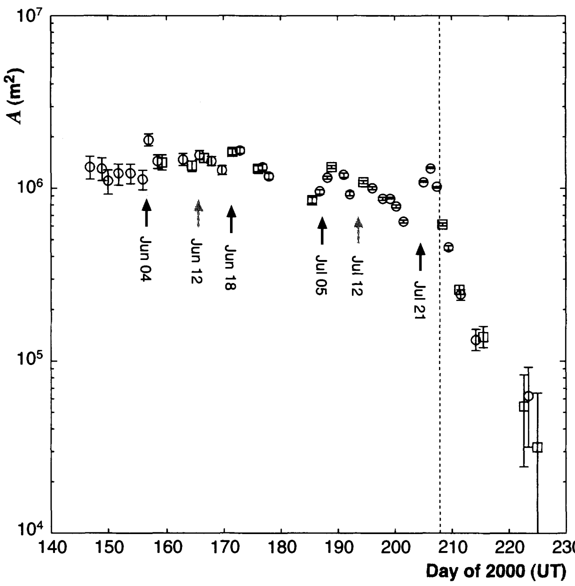

Fig. 3. Minimum cross section as a function of time. The cross section stays at the same level up to perihelion (dashed line), after which rapid dissipation is evident. Probable locations of disruptive events seen as a rapid increase of cross section are indicated by black arrows and potential events by gray arrows.

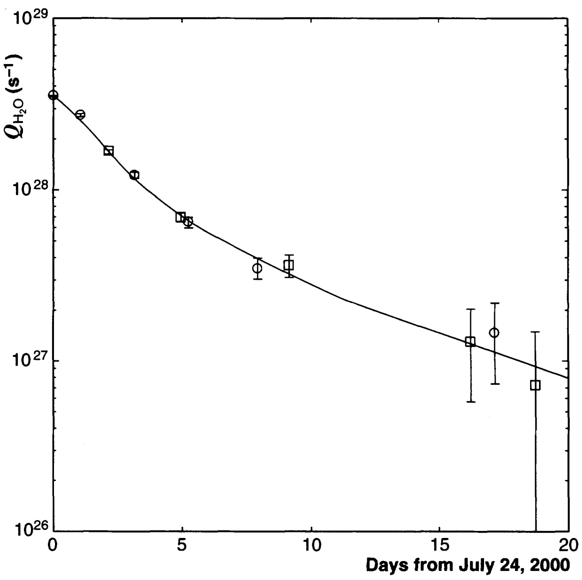

Fig. 4. Comparison of the water production of C/LINEAR during the final fragmentation event with a dissipation model. Observations are denoted by circles and squares, and the best fit of the model with parameters $M_0 = 3.25 \times 10^8$ kg, $\alpha = 2.74$, and $N_4/N_0 = 492$ is indicated with a solid line.

lengths (*10*, *11*) of a vectorial model (*12*). In addition, the comet-specific observations were analyzed with a more extensive Monte Carlo model (*13*). Both models gave similar water-production estimates because C/LINEAR did not produce a large flux of water, and so the H-atom velocity distribution was dominated by the photochemical kinetics of water and OH dissociation, rather than by collisional thermalization (*14*). The Q_{H_2O} as a function of heliocentric distance is shown in Fig. 2. The perihelion asymmetry is larger than with any comet observed in Lyman-alpha by IUE (International Ultraviolet Explorer) or SWAN. Integrating Q_{H_2O} over the period 25 May to 12 August 2000 yields $3.26 \pm 0.12 \times 10^9$ kg for the total mass of sublimated water.

The minimum sunward cross section of an icy body or bodies can be calculated from Q_{H_2O} if the sublimation is dominated by water, by requiring that the collected solar flux must provide at least enough energy to sublimate the observed amount of water (*15*). This effective area is shown as a function of time in Fig. 3. The area remains nearly constant at about 1 km^2 (except for a few brief outbursts) until the final disruption just before perihelion, after which the area decreases rapidly in accordance with sublimation of the remaining near-surface cometary water. Outburst events are also visible on 3 to 4, 12 to 13, and 17 to 19 June and 5 to 7 and 12 July. A huge increase in production rates could be seen in small-aperture observations (*16*, *17*) with a peak value nearly a factor of 4 larger than our Q_{H_2O} determined for 9 July. However, this difference may be due to a rapid increase in water production (possibly from small short-lived particles) whose integrated effect in the entire H coma is small. A classical explanation for such outbursts from comets when seen at large distances from the Sun is the presence of pockets of CO ice, which is much more volatile than water ice. This comet, however, is depleted in CO (*18*), and the detection of an expelled fragment connected to the 5 to 7 July event (*18*) indicates that a more probable cause for increases in water-production rates is successive fragmentation combined with ejection of gas and particulate matter from the freshly exposed surface.

The final dissipation of the comet after 24 July was modeled by assuming that a distribution of roughly spherical fragments with a homogeneous composition was produced during the event. A model with a distribution of fragments (*19*) following a power law $N(R) \sim \rho^2(R)R^{-\alpha}$, where N is the number of fragments, R and ρ are the particle radius and density, and $\alpha = 2.72 \pm 0.60$, agrees with the observed values (Fig. 4). Similar results have been obtained from ground-based observations (*16*). The derived power law has also been found to extend to microscopic particles (*17*) whose contribution cannot be detected by SWAN. If the bulk density of macroscopic fragments is assumed to be constant, $N(R)$ comes close to the distribution common in fractal or collisional distributions for cometary dust-tail particle sizes or planetesimal sizes. Because of the time-averaging nature of SWAN observations, this distribution corresponds to particles of centimeter size and larger. The distribution could be extended to smaller particles, which do not live long and do not produce much water, but would account for the rapid short-term water-production increase and subsequent decrease seen in the small-aperture instruments (*16*, *17*). The model gives the initial mass of water in the fragments available for sublimation on 24 July as $M_0 = 3.51 \pm 0.44 \times 10^8$ kg, which is a small value representing about 10% of the total water lost during the entire observing period. The model also suggests that Q_{H_2O} drops rapidly when all of the water in the largest original fragments sublimates completely. This model considers particles to completely sublimate, but the obtained results—size distribution and total mass—are fairly independent of actual properties of the particles, which could as well consist of refractory material thinly coated in ice (*20*).

The total volume of fragments observed by Hubble Space Telescope on 5 August was about 2×10^{-3} km^3 (*18*). According to our model, only the largest original fragments had not yet dissipated completely by that time, still possessing some 2.97×10^7 kg of water ice. Assuming that the nucleus was roughly homogeneous, this yields an estimate of 0.222 km^3 for the volume of the nucleus on 25 May, and a radius of 0.375 km. Comparing this to the determined Q_{H_2O}, we obtain an average preperihelion erosion rate of 3.3 m a day, which is an enormous value. It implies that from May to July, material was leaving the surface by fragmentation, rather than by direct sublimation. Considering the shape of the activity curve, it appears that the expelled material had the same characteristics as the fragments seen in the final event. This suggests that the observed activity of C/LINEAR was dominated by fragments that accounted for over one-half of the preperihelion water production.

It is also possible that the final fragmentation of the nucleus revealed its original constituents, and thus the size distribution reflects the actual structure of the nucleus. The fragile nature of the nucleus of C/LINEAR, combined with its lack of volatiles (*18*), tells us something important about its past history that makes it different in behavior from otherwise dynamically similar (i.e., highly inclined and large aphelion orbits) Oort cloud comets such as C/1996 B2 (Hyakutake) or C/1995 O1 (Hale-Bopp). It might alternatively be interpreted as indicating that this comet has been heavily processed from a previous passage or catastrophic event (*21*), or that it might be on its first pass through the inner solar system but formed in the warmer inner part of the solar nebula, affecting both its physical structure and its volatile composition.

Table 1. SWAN observations of C/LINEAR with tabulated values for the heliocentric r and SOHO-centric distances Δ and water-production rates Q_{H_2O}. The type of an observation is either full sky (s) or comet specific (c).

Month	Day	Hour (UT)	r (AU)	Δc (AU)	Q_{H_2O} (10^{28} s^{-1})	Type
May	25	18.0	1.3646	2.1264	1.13 ± 0.17	s
May	27	21.2	1.3351	2.0715	1.16 ± 0.17	s
May	28	22.7	1.3205	2.0435	1.01 ± 0.16	s
May	30	15.4	1.2973	1.9981	1.15 ± 0.16	s
June	1	18.3	1.2683	1.9398	1.20 ± 0.16	s
June	3	21.1	1.2397	1.8800	1.17 ± 0.16	s
June	4	22.7	1.2252	1.8492	2.02 ± 0.15	s
June	6	15.5	1.2024	1.7994	1.58 ± 0.14	s
June	7	07.0	1.1938	1.7802	1.57 ± 0.16	c
June	10	21.5	1.1461	1.6703	1.78 ± 0.13	s
June	12	14.3	1.1239	1.6169	1.70 ± 0.13	c
June	13	22.2	1.1068	1.5745	2.04 ± 0.12	s
June	14	14.2	1.0982	1.5530	1.98 ± 0.12	c
June	16	01.1	1.0797	1.5056	1.98 ± 0.11	s
June	17	23.7	1.0555	1.4413	1.81 ± 0.11	s
June	19	15.2	1.0352	1.3858	2.40 ± 0.11	c
June	21	00.3	1.0184	1.3386	2.55 ± 0.10	s
June	24	05.3	0.9806	1.2269	2.14 ± 0.09	c
June	25	00.0	0.9717	1.1996	2.23 ± 0.09	s
June	26	01.3	0.9598	1.1619	2.03 ± 0.09	s
July	3	13.8	0.8818	0.8895	1.76 ± 0.07	c
July	4	23.7	0.8688	0.8379	2.01 ± 0.07	s
July	6	09.4	0.8564	0.7869	2.49 ± 0.07	s
July	6	23.7	0.8514	0.7653	2.91 ± 0.07	c
July	9	05.2	0.8335	0.6858	2.72 ± 0.06	s
July	10	06.8	0.8255	0.6484	2.17 ± 0.06	s
July	12	13.5	0.8100	0.5716	2.64 ± 0.05	c
July	14	01.8	0.8009	0.5237	2.49 ± 0.05	s
July	16	03.5	0.7899	0.4643	2.21 ± 0.04	s
July	17	05.6	0.7849	0.4370	2.26 ± 0.04	s
July	18	06.9	0.7805	0.4139	2.06 ± 0.04	s
July	19	13.9	0.7759	0.3910	1.70 ± 0.04	s
July	23	00.8	0.7674	0.3660	2.94 ± 0.04	s
July	24	10.5	0.7658	0.3731	3.55 ± 0.04	s
July	25	11.6	0.7651	0.3847	2.74 ± 0.04	s
July	26	13.5	0.7650	0.4018	1.68 ± 0.04	c
July	27	13.3	0.7655	0.4215	1.22 ± 0.04	s
July	29	09.4	0.7676	0.4662	0.70 ± 0.05	c
July	29	15.5	0.7680	0.4731	0.65 ± 0.05	s
August	1	09.2	0.7747	0.5549	0.35 ± 0.05	s
August	2	13.5	0.7787	0.5936	0.37 ± 0.05	c
August	9	15.7	0.8158	0.8447	0.13 ± 0.07	c
August	10	14.4	0.8223	0.8791	0.15 ± 0.07	s
August	12	04.3	0.8340	0.9365	0.07 ± 0.08	c

References and Notes

1. J. H. Oort, *Bull. Astron. Inst. Neth.* **11**, 91 (1950).
2. J. L. Bertaux *et al.*, *Solar Phys.* **162**, 403 (1995).
3. J. L. Bertaux *et al.*, *Space Sci. Rev.* **87**, 129 (1999).
4. J. T. T. Mäkinen *et al.*, *Nature* **405**, 321 (2000).
5. J. T. T. Mäkinen *et al.*, *Astron. Astrophys.* **368**, 292 (2001).
6. The coma of this comet is too tenuous for an appreciable fraction of H atoms to become thermalized. Therefore, an adequate approach is to treat neutral H as two separate populations with different radial velocities, created by photodissociation of H_2O and OH, respectively.
7. The solar Lyman-alpha output varies by about 10% during one solar rotation, and this variation is directly transferred to the fluorescent intensity of cometary neutral H.
8. L. Haser, *Bull. Acad. R. Belg. Classe Sci.* **43**, 740 (1957).
9. The most important photodissociation chain, $H_2O + h\nu \rightarrow H + OH$ and $OH + h\nu \rightarrow O + H$, is simulated in the spherically symmetric model of expanding gas. An intensity profile is obtained from the calculated column densities and compared with the observed profile. χ^2 error estimates are obtained from the singular value decomposition method, which is used to fit the model to the data [for a description of the method see, e.g., (*22*)]. The H densities for the two H populations are given by

$$n_{H1}(r) = (Q_{H_2O}/4\pi v_{H1} r^2)\,[\gamma_{H_2O}/(\gamma_{H_1} - \gamma_{H_2O})]\,[\exp(-\gamma_{H_2O} r) - \exp(-\gamma_{H_1} r)]$$

and

$$n_{H2}(r) = (Q_{H_2O}/4\pi v_{H2} r^2)[A\exp(-\gamma_{H_2O} r) + B\exp(-\gamma_{H2} r) + C\exp(-\gamma_{OH} r)]$$

where v_i are the velocities and γ_i the inverse scale lengths of each species. The constants in the second formula are

$$A = [\gamma_{H_2O}/(\gamma_{H2} - \gamma_{H_2O})][1 + (\gamma_{H_2O})/(\gamma_{OH} - \gamma_{H_2O})]$$

$$B = -A + [\gamma_{H_2O}\gamma_{OH}/(\gamma_{OH} - \gamma_{H_2O})(\gamma_{H2} - \gamma_{OH})]$$

and $C = -A - B$.

10. M. R. Combi, A. H. Delsemme, *Astrophys. J.* **237**, 633 (1980).
11. The 1-AU scale lengths and velocities appropriate for solar maximum conditions were $\Lambda_{H_2O} = 6.6 \times 10^4$ km, $\Lambda_{OH} = 1.75 \times 10^5$ km, $\Lambda_{H1} = 3 \times 10^7$ km, $v_{H1} = 20$ km s^{-1}, $\Lambda_{H2} = 1.2 \times 10^7$ km, and $v_{H2} = 8$ km s^{-1}. Because of the large FOV, the inner production region of the H coma is not resolved, and so the calculations are more sensitive to the H velocities than to parent lifetimes.
12. M. C. Festou, *Astron. Astrophys.* **95**, 69 (1981).
13. M. R. Combi *et al.*, *Earth Moon Planets* **79**, 275 (1997).
14. The model neglects several minor effects like radiation pressure, Greenstein effect, and the dependence of scale lengths of different species on variations of the solar irradiation flux. Their combined contribution to the results can be estimated from given error margins.
15. This is similar but not equal to the active area and is defined as $A = LQr^2/[N_A F_S(1 - A_V)]$, where $L = 50$ kJ mol^{-1} is the latent heat of water for sublimation, r is the heliocentric distance in AU, $N_A = 6.022 \times 10^{23}$ mol^{-1} (the Avogadro constant), $F_S = 1365$ W m^{-2} (the solar constant), and $A_V = 0.03$ (the assumed Bond albedo of the nucleus). See, e.g., (*23*), for a discussion of this definition.
16. D. Bockelée-Morvan *et al.*, *Science* **292**, 1339 (2001).
17. T. L. Farnham *et al.*, *Science* **292**, 1348 (2001).
18. H. A. Weaver *et al.*, *Science* **292**, 1329 (2001).
19. The continuous size distribution is discretized by dividing it into classes of fragments of the same size. For the purpose of evaluation here, five particle-size groupings were used. For each class the total water-production rate Q_i of the class i can be obtained by solving the dissipation equation

$$dQ_i/dt = -(9u\sqrt{\pi N_i}/\rho)[N_A F_S(1 - A_V)/Lr^2]^{3/2}[Q_i(t)]^{1/2}$$

where $u = 1.66 \times 10^{-27}$ kg is the atomic mass unit, $N_i = N_0 b^{i/m}$, $i = 0, \ldots, m$ the number of fragments in the respective class, $b = N_m/N_0$, and ρ is the bulk density, which can be determined if N_0 is known or vice versa. The total water-production rate is thus $Q_{H_2O}(t) = \Sigma Q_i(t)$.
20. The initial mass on 24 July corresponds to the integrated loss of water after that point, and the power-law exponent determines the shape of the slope. It can thus be seen from Fig. 4 that the model reproduces these two quantities.
21. Z. Sekanina, *Astron. Astrophys.* **318**, L5 (1997).
22. W. H. Press, B. P. Flannery, S. A. Teukolsky, W. T. Vetterling, *Numerical Recipes* (Cambridge Univ. Press, New York, 1986), pp. 52–64.
23. H. U. Keller, in *Physics and Chemistry of Comets*, W. F. Huebner, Ed. (Springer-Verlag, Berlin, 1990), pp. 18–21.
24. SOHO is an international cooperative mission of the European Space Agency and NASA. SWAN was financed by Centre National d'Études Spatiales (France) with support from CNRS and by Teknologian Kehittämiskeskus (National Technology Agency, Finland) and the Finnish Meteorological Institute. J.T.T.M. was supported by the Academy of Finland. M.R.C. acknowledges support from the SOHO Guest Investigator Programme. We thank the authors of the other C/LINEAR papers in this issue for sharing their results before publication, especially H. A. Weaver for constructive comments.

20 March 2001; accepted 19 April 2001

HST and VLT Investigations of the Fragments of Comet C/1999 S4 (LINEAR)

H. A. Weaver,[1*] Z. Sekanina,[2] I. Toth,[3] C. E. Delahodde,[4†] O. R. Hainaut,[4] P. L. Lamy,[5] J. M. Bauer,[6] M. F. A'Hearn,[7] C. Arpigny,[8] M. R. Combi,[9] J. K. Davies,[10] P. D. Feldman,[1] M. C. Festou,[11] R. Hook,[12] L. Jorda,[5] M. S. W. Keesey,[2] C. M. Lisse,[13‡] B. G. Marsden,[14] K. J. Meech,[6] G. P. Tozzi,[15] R. West[12]

At least 16 fragments were detected in images of comet C/1999 S4 (LINEAR) taken on 5 August 2000 with the Hubble Space Telescope (HST) and on 6 August with the Very Large Telescope (VLT). Photometric analysis of the fragments indicates that the largest ones have effective spherical diameters of about 100 meters, which implies that the total mass in the observed fragments was about 2×10^9 kilograms. The comet's dust tail, which was the most prominent optical feature in August, was produced during a major fragmentation event, whose activity peaked on UT 22.8 ± 0.2 July 2000. The mass of small particles (diameters less than about 230 micrometers) in the tail was about 4×10^8 kilograms, which is comparable to the mass contained in a large fragment and to the total mass lost from water sublimation after 21 July 2000 (about 3×10^8 kilograms). HST spectroscopic observations during 5 and 6 July 2000 demonstrate that the nucleus contained little carbon monoxide ice (ratio of carbon monoxide to water is less than or equal to 0.4%), which suggests that this volatile species did not play a role in the fragmentation of C/1999 S4 (LINEAR).

Cometary fragmentation events provide an opportunity to gather direct information on the internal structure and composition of cometary nuclei, which is difficult to obtain in any other way. Optical imaging observations of comets suggest that their nuclei split at a rate of at least once every hundred years (*1*). These fragmentations are generally grouped into two categories: events that seem to be caused by tidal interactions with a nearby large object, such as for comet D/Shoemaker-Levy 9 after its close approach to Jupiter in 1992, and disruptions that occur for no apparent reason, although breakup due to fast rotation is a tenable explanation in at least some of these cases (*2–4*). The nucleus of comet C/1999 S4 (LINEAR), hereafter called C/LINEAR, underwent multiple fragmentations during its recent apparition, culminating in the complete disruption of its nucleus during the latter part of July 2000 (*5*). C/LINEAR did not pass particularly close to any major planetary body during its current apparition, so tidal disruption is apparently not responsible for its fragmentation.

C/LINEAR was discovered on 27 September 1999 (all dates are expressed in universal time) by the Lincoln Near Earth Asteroid Research (LINEAR) program (*6*) at a heliocentric distance of 4.3 astronomical units (AU) (1 AU = 1.496×10^{11} m is the average Earth-Sun distance). The comet was apparently on its first visit to the inner solar system from the Oort cloud, a vast reservoir of $\sim 10^{12}$ comets that surrounds the Sun (*7, 8*), and reached perihelion on 26 July 2000 at a heliocentric distance of 0.77 AU. We observed C/LINEAR both pre-

[1]Department of Physics and Astronomy, Johns Hopkins University, 3400 North Charles Street, Baltimore, MD 21218–2686, USA. [2]Jet Propulsion Laboratory, 4800 Oak Grove Drive, Pasadena, CA 91109, USA. [3]Konkoly Observatory, Post Office Box 67, Budapest H–1525, Hungary. [4]European Southern Observatory, Alonso de Cordova 3107, Santiago, Chile. [5]Laboratoire d'Astronomie Spatiale du CNRS, BP 8, 13376 Marseille, Cedex 12, France. [6]Institute for Astronomy, University of Hawaii, 2680 Woodlawn Drive, Honolulu, HI 96822, USA. [7]Department of Astronomy, University of Maryland, College Park, MD 20742, USA. [8]Institut d'Astrophysique, Université de Liège, B-4000 Liège, Belgium. [9]Space Physics Research Laboratory, University of Michigan, 2455 Hayward Street, Ann Arbor, MI 48109–2143, USA. [10]Joint Astronomy Centre, Hilo, HI 96720, USA. [11]Observatoire Midi-Pyrénées, 14 avenue Edouard Belin, F-31400, Toulouse, France. [12]European Southern Observatory, Karl-Schwarzschild-Strasse 2, D-85748 Garching, Germany. [13]Space Telescope Science Institute, 3900 San Martin Drive, Baltimore, MD 21218, USA. [14]Smithsonian Astrophysical Observatory, 60 Garden Street, Cambridge, MA 02138, USA. [15]Osservatorio Astrofisico di Arcetri, Largo E. Fermi 5, I-50125, Florence, Italy.

*To whom correspondence should be addressed.
†Present address: Laboratoire d'Astronomie Spatiale du CNRS, BP 8, 13376 Marseille, Cedex 12, France.
‡Present address: Department of Astronomy, University of Maryland, College Park, MD 20742, USA.